NMR study of InP quantum dots: Surface structure and size effects

M. Tomaselli, J. L. Yarger, M. Bruchez Jr., R. H. Havlin, D. deGraw, A. Pines, and A. P. Alivisatos

Citation: The Journal of Chemical Physics **110**, 8861 (1999); doi: 10.1063/1.478858
View online: http://dx.doi.org/10.1063/1.478858
View Table of Contents: http://scitation.aip.org/content/aip/journal/jcp/110/18?ver=pdfcov
Published by the AIP Publishing

NMR study of InP quantum dots: Surface structure and size effects

M. Tomaselli, J. L. Yarger, M. Bruchez, Jr., R. H. Havlin, D. deGraw, A. Pines, and A. P. Alivisatos
Materials Sciences Division, Lawrence Berkeley National Laboratory, Berkeley, California 94720 and Department of Chemistry, University of California, Berkeley, California, 94720

(Received 22 December 1998; accepted 5 March 1999)

We report the results of ^{31}P NMR measurements on trioctylphosphine oxide (TOPO) passivated InP quantum dots. The spectra show distinct surface-capping sites, implying a manifold of crystal–ligand bonding configurations. Two In ^{31}P surface components are resolved and related to different electronic surroundings. With decreasing particle size the In ^{31}P core resonance reveals an increasing upfield chemical shift related to the overall size dependence of the InP electronic structure. © *1999 American Institute of Physics.* [S0021-9606(99)70718-X]

Semiconductor clusters with monodisperse diameters ranging from 10–100 Å manifest quantum dot behavior.[1] The surface composition of these colloidally prepared particles[2] has been shown to be important because of its influence on the discrete electronic structure and quantum confinement[1,3–5] as well as its relation to electronic transport properties,[1,6] structural phase transitions, and thermodynamic stability.[7] In addition, the spectroscopic characterization of the capping molecules can provide valuable information on the morphology and faceting[1] of the nanoparticles.

In this letter, we report an initial study on III–V semiconductor InP dots using one- and two-dimensional (1D and 2D) NMR. We find distinct capping and In ^{31}P surface sites, implying a variety of ligand–crystal bonding arrangements and structural environments. The chemical shielding of the In ^{31}P resonance increases with decreasing dot size which can be interpreted as a decrease in the ^{31}P paramagnetic shift with increasing electronic excitation energy of the quantum-confined nanoparticles.

InP samples have been prepared under argon using the dehalosilation reaction of $InCl_3$ and $P(Si(CH_3)_3)_3$ at 540–570 K in TOPO as coordinating solvent.[8] Distinct size distributions of the particles were obtained by size-selective precipitation resulting in InP clusters with average diameters in the range of 20–50 Å and distributions of ~20%.[8] For the surface selective experiments, the separation and isolation were carried out in a drybox. The precipitates were dried under vacuum and the resulting powder samples sealed in pyrex tubes (0.13 Pa). In a second synthesis, the identical precipitation and isolation procedure was carried out in air, yielding TOPO and oxide passivated InP dots.[1,8] X-ray diffraction spectra (Siemens D5000, Cu K_α radiation) and transmission electron microscopy images (TEM, TopCon EM002B) showed that the InP dots were highly crystalline (pure phase, zinc-blende), roughly spherical in shape, with indications of faceting. The cluster diameters (d) were inferred from UV/vis absorption spectra (HP 8452) obtained immediately upon separation.[8]

Figures 1(A) and 1(B) show typical 1D ^{31}P ($S=1/2$) NMR spectra of TOPO-InP ($d \simeq 45$ Å) recorded under conditions of magic-angle spinning (MAS).[9] The experiments were performed at a ^{31}P Larmor frequency of $\nu_0 = 75.18$ MHz ($B_0 = 4.36$ T) and $\nu_0 = 161.99$ MHz ($B_0 = 9.39$ T) using Chemagnetics CMX spectrometers and 4 mm MAS probe assemblies from the same manufacturer. The MAS frequency (ν_{mas}) was stabilized within 3 Hz for all experiments. The B_1 nutation frequency was matched to $\nu_1 = 140$ kHz on all channels (^{1}H,^{31}P,^{13}C). Spectrum 1(A) was obtained by a ^{31}P single-pulse excitation with ^{1}H decoupling during data acquisition. The inhomogeneously broadened resonance at -178 ppm (relative to 85% H_3PO_4) with a linewidth of $\delta_{1/2} = 58$ ppm ($\nu_{1/2} = 4400$ Hz) is assigned to the In ^{31}P core (interior) nuclei: For a spherical InP cluster with a typical diameter of 45 Å, only ~20% of all atoms reside at the surface. The lineshape is slightly asymmetric and upfield shifted with respect to bulk In ^{31}P [$\delta = -147$ ppm, $\delta_{1/2} = 43$ ppm ($\nu_{1/2} = 3200$ Hz)], with the main source of broadening being the indirect exchange interaction with the ^{115}In neighbors ($S=9/2$),[10] as well as a contribution from the second-order anisotropic (pseudo)dipolar–quadrupolar shift.[11,12] The weak downfield segment of the spectrum (~8%) in the range $-20 < \delta < 80$ ppm corresponds to ^{31}P TOPO resonances at the crystal surface. From the relative

TABLE I. ^{31}P chemical-shift parameters (75.18 MHz, 300 K); δ_{aniso} is the anisotropy and η the asymmetry of the chemical-shift anisotropy tensor (CSA) as defined in Ref. 18.

	δ_{iso} (ppm)	$\delta_{1/2}^{mas}$ (ppm)	δ^{a}_{aniso} (ppm)	η^{a}
Free TOPO	47	2	118±3	0±0.05
InP-TOPO1	71±2	10±2	96±5	0±0.1
InP-TOPO2	36±2	12±2	…[b]	…[b]
InP-TOPO3	6±2	10±2	78±6	1±0.1
InP-TOPO4	−8±2	12±2	…[b]	…[b]
InP (bulk)	−147[c]	43[c]	0[c]	0[c]
InP-core (45 Å)	−178±4[d]	58±5[d]		
α-InP (45 Å)	−118±8[d]	63±7[d]		
β-InP (45 Å)	−199±6[d]	55±5[d]		

[a]Static CP and MAS rotary-resonance (Ref. 19) data.
[b]Motionally averaged CSA; $\delta_{1/2}^{static} = 24 \pm 5$ ppm.
[c]Undopted material; (Ref. 10).
[d]Lorentzian least-squares fit.

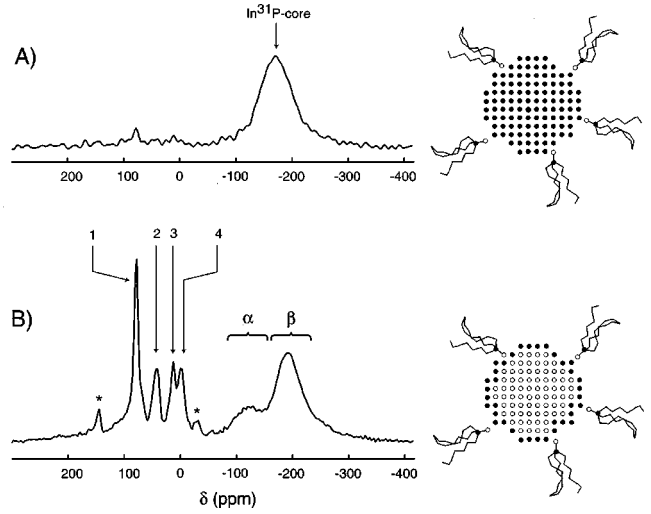

FIG. 1. 1D ^{31}P NMR spectra of TOPO-InP dots ($d \simeq 45$ Å) recorded at 75.18 MHz and 300 K (~5 mg sample sealed in a pyrex tube). (A) Single pulse experiment; 300 s delay between experiments; 256 transients. (B) Surface selective ^{1}H→^{31}P cross-polarization experiment with $\tau_{cp}=300\ \mu$s; 1.5 s delay between experiments; 36 000 transients. Both experiments were recorded under MAS ($\nu_{mas}=5$ kHz) and on-resonance ^{1}H decoupling during data acquisition. Spinning sidebands are marked with asterisks. The labeled resonances are described in the main text.

intensities of the two components in Fig. 1(A) we infer an average TOPO surface coverage of ~20%, consistent with x-ray photoelectron spectroscopy (XPS) on similar samples.[8] Spectrum 1(B) was obtained by ^{1}H→^{31}P cross polarization (CP)[13] with a contact time of $\tau_{cp}=300\ \mu$s and proton decoupling during data acquisition. The lineshape in Fig. 1(B) differs considerably from that of Fig. 1(A) since the CP experiment probes ^{31}P spins in close proximity to the TOPO protons and is therefore *surface selective*. Four different ^{31}P capping resonances are resolved (TOPO 1–4) with isotropic chemical shifts (δ_{iso}) at 71, 36, 6, and −8 ppm and an average linewidth of 11 ppm (relative intensity ratios: 1.0:0.4:0.3:0.3). The distribution of chemical shift parameters (see Table I) implies a manifold of ligand–crystal bonding environments [i.e., unidentate and bridging oxygen coordination[14] to the cation (In) or perhaps anion (P)].[8] This indicates that the capping molecules occupy distinct InP-surface sites, conceivably due to the faceting of the nanoparticles. Our finding contrasts with earlier studies on thiophenol capped CdS or TOPO/TOP capped CdSe particles where only one surfactant site was identified.[15]

The upfield part of the spectrum in Fig. 1(B) shows two partially overlapping In-bonded ^{31}P resonances centered at −118 ppm (α-InP) and −199 ppm (β-InP). Both lines are shifted with respect to the core resonance [see Fig. 1(A)] and they can be interpreted as two different structural In ^{31}P-surface environments. The assignment is corroborated by a series of CP experiments with varying contact time (Fig. 2): We find a gradual downfield shift of the first moment for $\tau_{cp}>0.5$ ms (dashed line in Fig. 2). This can be rationalized by the presence of a slow polarization-transfer process from TOPO protons to remote ^{31}P core nuclei, shifted in resonance frequency with respect to ^{31}P surface spins. Neglecting chemical-shift differences among the core nuclei, the full series of CP spectra is fitted quite well with a minimum of three Lorentzian components with varying intensities but constant chemical shifts and linewidths (Fig. 2 and Table I). The dependence of the extracted intensities as a function of τ_{cp} is shown in Fig. 2, with the curves fitted by the form $M_{qe}(1-e^{-\tau_{cp}/T_{IS}})$ invoking the spin-temperature approximation and neglecting $T_{1\rho}$ relaxation.[9,16] It is evident that the surface components (α, β-InP, and TOPO) reach a state of quasi-equilibrium for $\tau_{cp}>1.5$ ms and are characterized by buildup rates roughly one order-of-magnitude faster than that of the core spins. For the present experimental conditions (i.e., high spinning speed where the *IS* zero-quantum linewidth is given by the effective *IS* dipolar coupling frequency),[17] $T_{IS}\propto\langle r_{IS}^{3}\rangle$. Here, r_{IS} denotes a typical distance between ^{31}P spins and surface protons. Assuming that the TOPO ^{31}P nuclei are efficiently polarized by the nearest-

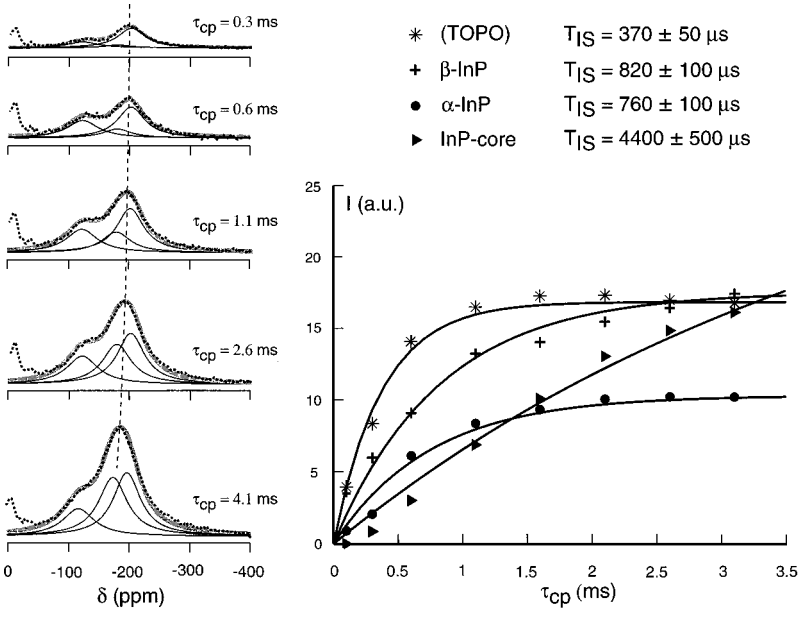

FIG. 2. Left side: 1D ^{1}H→^{31}P CP spectra of TOPO-InP dots with varying τ_{cp}: 2 s delay between scans; 18 000 transients. Other experimental parameters are as in Fig. 1(B). Only the indium-bonded portion of the ^{31}P spectra is shown (dotted line: experiment, gray line: least-squares Lorentzian fit described in the main text). The vertical dashed curve connects the spectral maxima, emphasizing the downfield shift of the first moment with increasing τ_{cp}. Right side: Buildup of the ^{31}P intensities with increasing τ_{cp}. The extracted time constants (T_{IS}) are given in the figure.

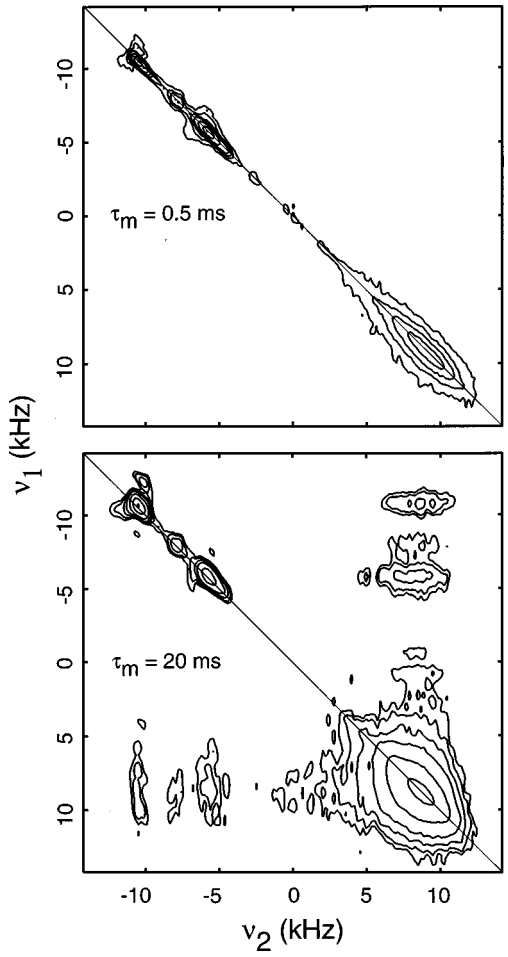

FIG. 3. 2D ^{31}P correlation spectra of TOPO/oxide passivated InP clusters (Ref. 20) ($d \simeq 32$ Å) recorded with $\tau_{cp}=5$ ms ($\nu_{mas}=10$ kHz). Similar spectra were recorded for TOPO-InP with $d \simeq 45$ Å. Protons were decoupled during the evolution (t_1), detection (t_2), and mixing (τ_m) times; 1024 transients per t_1 value. The data sets (100×100 points) were zero filled to 256 points in each dimension and Fourier transformed to obtain pure absorption mode spectra. ^{31}P spin diffusion was driven by rotor-synchronized 180° radio-frequency (rf) pulses during the mixing time (Ref. 21) and is manifested by the occurrence of cross peaks ($\nu_1 \neq \nu_2$) connecting the various sites on the diagonal (thin lines). Contours are at 4%, 6%, 16%, 32%, 64%, and 96% of the maximum signals.

neighbor protons only (i.e., $\langle r_{IS}\rangle_{intra}=2.5$ Å), a lower bound for the ^{1}H–^{31}P distances can be estimated: We obtain $\langle r_{IS}\rangle_{\alpha,\beta} \simeq 3.2$ Å (a typical H–P van der Waals distance) and $\langle r_{IS}\rangle_{core} \simeq 6$ Å, indicating that the capping octyl chains are in closest contact with the semiconductor surface. This conclusion is further corroborated by the observed upfield shift of 3 ppm for the InP-TOPO $^{13}CH_2$ resonances compared to free TOPO. Moreover, the core spins probed by the CP experiment with $0.5<\tau_{cp}<4$ ms reside within the first and second shell from the crystal surface. For $\tau_{cp}>50$ ms the CP spectra converge to the single-pulse spectrum shown in Fig. 1(A). In fact, fitting spectrum 1(A) with the parameters given in Table I results in a relative InP-surface fraction (α,β-InP) of 24%, in agreement with the previous estimate of ~20%.

The spatial proximity of the various ^{31}P sites can be probed by 2D rf driven spin-diffusion experiments[17,21] (Fig. 3). Since the rate of the dipole induced mutual spin flips strongly depends on the nuclear separation (r_{ij}^{-3}),[17] spin diffusion is almost exclusively confined to neighboring ^{31}P species. As expected, the spectra show no cross peaks due to spin diffusion for short mixing times ($\tau_m=0.5$ ms). Nevertheless, the inhomogeneous character of the ^{31}P spectrum is clearly exposed by the elongated shape of the signal peaks along the diagonal. At longer times of several tens of milliseconds, cross peaks between all surface sites and the In ^{31}P core emerge. The asymmetry of the intensities across the diagonal indicates a preferential surface→core directed spin-diffusion process. No polarization transfer among the various capping resonances could be detected on time scales of $0.1<\tau_m<200$ ms under MAS or static conditions. This indicates no aggregation of capping molecules on the cluster surface for $d>30$ Å. Furthermore, broadband[21,22] as well as frequency selective[17] spin-diffusion experiments suggest that the spectral features observed in the 1D data mainly result from structural variations within the clusters, although contributions of heterogeneities induced by the particle size distribution cannot be completely excluded. In particular, in proton driven spin-diffusion experiments[17] with $2<\tau_m<60$ ms (data not shown) we find that the α-InP site exhibits a rapid polarization transfer to the core and β fraction, but does not sample its own local environment. Consequently, α-^{31}P surface sites share similar electronic surroundings but are spatially remote from each other. Since XPS data indicate that the large majority of TOPO ligands bind to indium,[8] both In ^{31}P surface species can be regarded as uncapped. Based on the relative chemical-shift differences, we therefore conclude that the β-InP fraction reflects a relatively ''unperturbed'' core-like nearest-neighbor configuration, whereas α-In ^{31}P nuclei manifest significantly altered bonding environments, possibly due to surface reconstruction to reduce the number of dangling bonds.

The electronic quantum confinement of the InP particles is reflected by the ^{31}P chemical shift data: In analogy with experiments on II–VI clusters,[23] we find an increasing upfield shift with decreasing dot size. Figure 4 illustrates this behavior by correlating the chemical shift with the inverse energy corresponding to the average size-dependent band gap of the clusters. Since size variations in the electronic structure arise through systematic transformations in the density of states[1,3] (i.e., the electronic states shift to higher energy with the concentration of the oscillator strength into a few transitions), it is surmised that the observed drift in the chemical shift is largely dominated by the paramagnetic contribution (σ_p) to the chemical shielding interaction.[24] The isotropic value of σ_p can be expressed in a perturbation treatment as[24]

$$\sigma_p^{iso}=-\frac{\mu_0 e^2\hbar^2}{8m_e^2\pi}\sum_{n\neq 0}\frac{1}{\Delta E_n}\Bigg[\langle 0|\Sigma_l\frac{\partial}{\partial\phi_l}|n\rangle \times\langle n|\Sigma_{l'}\frac{\partial}{\partial\phi_{l'}}\frac{1}{q_{l'}^3}|0\rangle+\langle 0|\Sigma_{l'}\frac{\partial}{\partial\phi_{l'}}\frac{1}{q_{l'}^3}|n\rangle \times\langle n|\Sigma_l\frac{\partial}{\partial\phi_l}|0\rangle\Bigg]. \quad (1)$$

Here, m_e is the mass of the electron, q_l and ϕ_l are the dis-

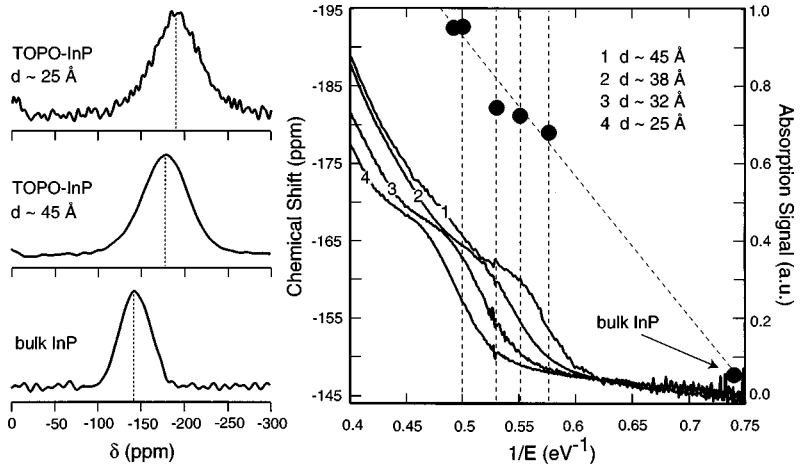

FIG. 4. Left side: 1D single pulse ^{31}P MAS spectra of bulk undoped InP and two TOPO/oxide passivated InP clusters of different diameters; 60 s delay between experiments; $\nu_{mas}=10$ kHz. Right side: Plot of the extracted ^{31}P chemical shift values (circles) vs. inverse energy. The nanoparticle UV/vis absorption curves (300 K toluene) are also displayed for comparison. The chemical shift data is correlated with the inverse average band gap energy of the InP particles given by the point of inflection of the absorption curves (vertical dashed lines).

tance from the origin and the azimuthal angle that define the position of electron l in a spherical coordinate system centered at the nuclear spin with the z axis collinear with $\mathbf{B}_0$. Summing explicitly over all states n with electronic excitation energies ΔE_n is necessary for a rigorous calculation of σ_p. Qualitatively, Eq. (1) explains the experimental observation: With decreasing particle size, the electronic excitation energies ΔE_n increase and thereby reduce the downfield paramagnetic chemical shift. The graph in Fig. 4 implies the crude approximation that $\Delta E_1 \ll \Delta E_{n\neq 1}$. In this limit, the fairly linear relationship between the ^{31}P shift and the average inverse lattice band gap energy, extrapolated from the bulk, suggests that a change from ΔE_1 towards a limiting energy separation, more suitable for molecular systems, is not yet reached for an InP cluster with $d \simeq 25$ Å.

The results in this study are based upon the sensitivity of NMR to the local structure and electronic surroundings of the nuclear spins. A variety of surface components are identified and characterized using multinuclear polarization transfer and two-dimensional correlation techniques. We expect that the application of recent developments in *ab initio* and density functional methods for the calculation of magnetic resonance parameters[25] will complement and further elucidate our experimental observations in this new class of materials.

ACKNOWLEDGMENTS

This work was supported by the Director, Office of Energy Research, Office of Basic Energy Sciences, Materials Sciences Division, U.S. Department of Energy, under contract No. DE-AC03-76SF00098. J.L.Y., M.B., and R.H.H. acknowledge support from NSF research fellowships. M.T. acknowledges support from the Swiss National Science Foundation.

[1] L. E. Brus, J. Phys. Chem. **90**, 2555 (1986); A. P. Alivisatos, *ibid.* **100**, 13226 (1996).
[2] C. B. Murray, D. J. Norris, and M. G. Bawendi, J. Am. Chem. Soc. **115**, 8706 (1993).
[3] V. L. Colvin, A. P. Alivisatos, and J. G. Tobin, Phys. Rev. Lett. **66**, 2786 (1991); M. G. Bawendi, P. J. Carroll, W. L. Wilson, and L. E. Brus, J. Chem. Phys. **96**, 946 (1992).
[4] S.-H. Kim, R. H. Wolters, and J. R. Heath, J. Chem. Phys. **105**, 7957 (1996); O. I. Mićić, H. M. Cheong, H. Fu, A. Zunger, J. R. Sprague, A. Mascarenhas, and A. J. Nozik, J. Phys. Chem. **101**, 4904 (1997).
[5] H. Fu and A. Zunger, Phys. Rev. B **56**, 1496 (1997).
[6] D. L. Klein, P. L. McEuen, J. E. B. Katari, R. Roth, and A. P. Alivisatos, Appl. Phys. Lett. **68**, 2574 (1996).
[7] C.-C. Chen, A. B. Herold, C. S. Johnson, and A. P. Alivisatos, Science **276**, 398 (1997).
[8] A. A. Guzelian, J. E. B. Katari, A. V. Kadavanich, U. Banin, K. Hamad, E. Juban, P. Alivisatos, R. H. Wolters, C. C. Arnold, and J. R. Heath, J. Phys. Chem. **100**, 7212 (1996).
[9] M. Mehring, *Principles of High Resolution NMR in Solids* (Springer, Berlin, 1983).
[10] M. Tomaselli, D. deGraw, J. L. Yarger, M. P. Augustine, and A. Pines, Phys. Rev. B **58**, 8627 (1998).
[11] D. L. VanderHart, H. S. Gutowsky, and T. C. Farrar, J. Am. Chem. Soc. **89**, 5056 (1967).
[12] The ^{115}In NMR signals of the investigated particles were broadened beyond detectability due to quadrupolar couplings, possibly caused by slight bond strains and electric field gradients at or near the surface. Decoupling at the bulk ^{115}InP resonance frequency (Ref. 10) had no detectable narrowing effect on the ^{31}P lineshape.
[13] A. Pines, M. G. Gibby, and J. S. Waugh, J. Chem. Phys. **59**, 569 (1973).
[14] T. S. Lobana, in *The Chemistry of Organophosphorous Compounds Vol. 2*, edited by F. R. Hartley (Wiley, New York, 1992).
[15] J. R. Sachleben, E. W. Wooten, L. Emsley, A. Pines, V. L. Colvin, and A. P. Alivisatos, Chem. Phys. Lett. **198**, 431 (1992); L. R. Becerra, C. B. Murray, R. G. Griffin, and M. G. Bawendi, J. Chem. Phys. **100**, 3297 (1994).
[16] Since ν_{mas} exceeds the strongest ^{31}P–^{31}P dipolar coupling frequency, the homonuclear ^{31}P polarization transfer is negligible during the CP period.
[17] B. H. Meier, Adv. Magn. Opt. Reson. **18**, 1 (1994); S. M. De Paul, M. Tomaselli, A. Pines, M. Ernst, and B. H. Meier, J. Chem. Phys. **108**, 826 (1998).
[18] U. Haeberlen, *High Resolution NMR in Solids, Selective Averaging* (Academic, New York, 1976).
[19] Z. Gan, D. M. Grant, and R. R. Ernst, Chem. Phys. Lett. **254**, 349 (1996).
[20] TOPO/oxide passivated InP particles showed an additional $^{31}PO_4$-surface resonance at 5 ppm ($\delta_{1/2}^{mas}=15$ ppm). The assignment is based on $^1H\rightarrow{}^{13}C\rightarrow{}^{13}P$ double cross-polarization experiments.
[21] D. K. Sodickson, M. H. Levitt, S. Vega, and R. G. Griffin, J. Chem. Phys. **98**, 6742 (1993).
[22] M. Baldus, M. Tomaselli, B. H. Meier, and R. R. Ernst, Chem. Phys. Lett. **230**, 329 (1994).
[23] A. M. Thayer, M. L. Steigerwald, T. M. Duncan, and D. C. Douglass, Phys. Rev. Lett. **60**, 2673 (1988).
[24] N. F. Ramsey, Phys. Rev. **78**, 699 (1950).
[25] M. Schindler and W. Kutzelnigg, J. Chem. Phys. **76**, 1919 (1982); V. G. Malkin, O. L. Malkina, and D. R. Salahub, Chem. Phys. Lett. **204**, 80 (1993); F. Mauri, B. G. Pfrommer, and S. G. Louie, Phys. Rev. Lett. **77**, 5300 (1996).